Available online at www.sciencedirect.com

SCIENCE DIRECT®

Earth and Planetary Science Letters 228 (2004) 243–253

EPSL

www.elsevier.com/locate/epsl

Hemispherical transition of seismic attenuation at the top of the earth's inner core

Aimin Cao*, Barbara Romanowicz

Berkeley Seismological Laboratory, 215 McCone Hall, University of California, Berkeley, Berkeley, CA 94720-4760, United States

Received 24 May 2004; received in revised form 7 September 2004; accepted 15 September 2004

Editor: S. King

Abstract

In contrast to the liquid outer core, the earth's inner core is mostly solid, and its composition is more pure iron. Based on dynamic arguments related to the freezing process of the inner core, and the observation of much lower P-wave quality factor in the inner core (Q_α<450) than in the outer core (Q_α>10,000), it has been suggested that a mushy layer with liquid inclusions may exist at the top of the inner core. On the other hand, seismic measurements indicate that Q_α increases towards the center of the inner core. We here present estimates of Q_α in the depth range 32–110 km beneath the Inner Core Boundary (ICB), based on the measurement of PKIKP/PKiKP amplitude ratios after a narrow band-pass filtering (0.7–2.0 Hz). Our measurements indicate that there are pronounced hemispherical differences in the values of Q_α (~335 and ~160 in the western (180°W to 40°E) and eastern (40°E to 180°E) hemispheres, respectively), and in the depth of transition from decreasing to increasing Q_α (<32 km beneath the ICB in the eastern hemisphere and ~85 km in the western hemisphere). Below 85 km, the hemispherical pattern disappears. We also confirm the existence of a correlated hemispherical pattern in P velocity down to 85 km. The P velocity and Q_α variations are compatible with an interpretation in terms of small hemispherical variations of temperature at the top of the inner core and their influence on the morphology of porosity and connectivity of liquid inclusions in the mushy zone. The disappearance of the differences in Q_α beneath 85 km provide constraints on the likely depth extent of the mushy zone.

Keywords: attenuation; Q_α; inner core; PKIKP/PKiKP amplitude ratio

1. Introduction

The Earth's inner core is formed by a freezing process of iron as the liquid outer core gradually cools [1,2]. Because the outer core material is not pure iron [3,4], some of the light elements are excluded from the inner core during this dynamic process, to power the geodynamo [3,5–7], while the residual is likely kept within a mushy layer at the top of the inner core [8–11]. Thus, constraining the characteristics of the mushy layer at the top of the inner core, as revealed by seismic velocity and attenuation measurements,

* Corresponding author. Tel.: +1 510 642 6994; fax: +1 510 643 5811.

E-mail address: acao@seismo.berkeley.edu (A. Cao).

0012-821X/$ - see front matter © 2004 Elsevier B.V. All rights reserved.
doi:10.1016/j.epsl.2004.09.032

should give us important insights into the dynamics of the Earth's core.

Since the existence of seismic anisotropy in the inner core was first suggested [12,13], its proposed structure has become more complicated and more controversial. The P-wave velocity anisotropy could vary with depth [14–16]; in the 100–400 km depth range, there may be a very weakly anisotropic quasi-eastern hemisphere and an anisotropic quasi-western hemisphere for P-wave velocity [17,18] and attenuation [19,20]; at the top 80 km of the inner core, there may be an isotropic layer characterized by faster P-wave velocity in the quasi-eastern hemisphere than in the quasi-western hemisphere [21–23]. However, Romanowicz et al. [24] and Ishii et al. [25] questioned the above complexity. Ishii et al. [25] suggested that there might be no an isotropic layer at the top of the inner core and that constant anisotropy in the whole of the inner core may explain the bulk of the data. Bréger et al. [26] and Romanowicz et al. [24] suggested that the complex lateral variations of P-wave velocity could be due to structure elsewhere in the earth.

The outer core Q_α is usually regarded as infinite ($\geq$10,000) [27], but the estimated Q_α in the inner core is constrained to be less than 450 [28,29]. This huge contrast indicates that a zone of decreasing Q_α with depth must exist beneath the Inner Core Boundary (ICB) [9]. However, this zone of decreasing Q_α should be confined to the top of the inner core, because multiple seismic observations confirm that Q_α increases with depth below a depth of approximately 100 km beneath the ICB [30–32,11]. Therefore, the existence of a transition zone at the top of the inner core, where Q_α turns from decreasing to increasing with depth, seems likely.

In order to study the seismic structure at the top of the inner core, the most suitable body wave phases are PKIKP and PKiKP in the epicentral distance range from 120° to 144° (Fig. 1). In this distance range, PKIKP samples the top 0–110 km of the inner core and PKiKP is reflected from ICB. The two phases have almost the same ray paths in the mantle and very close ray paths in the outer core. Hence, the assumption that they experience almost the same heterogeneities in the mantle and outer core is valid in a first approximation [33,21–23]. The differences in travel times and amplitudes can therefore be attributed to the vicinity of the ICB.

Unfortunately, these two phases present a great challenge. The separation of PKIKP and PKiKP is very small. For example, it is less than 1.3 s when the epicentral distance is less than 135° (when referred to the seismic reference model PREM [28]; Fig. 2b). On the other hand, the source time functions are usually longer than 3.0 s for events of $m_b \geq 5.5$ [33]. Interference between the two phases seems inevitable.

In order to solve this problem, both Wen and Niu [23] and Garcia [22] adopted a waveform modeling

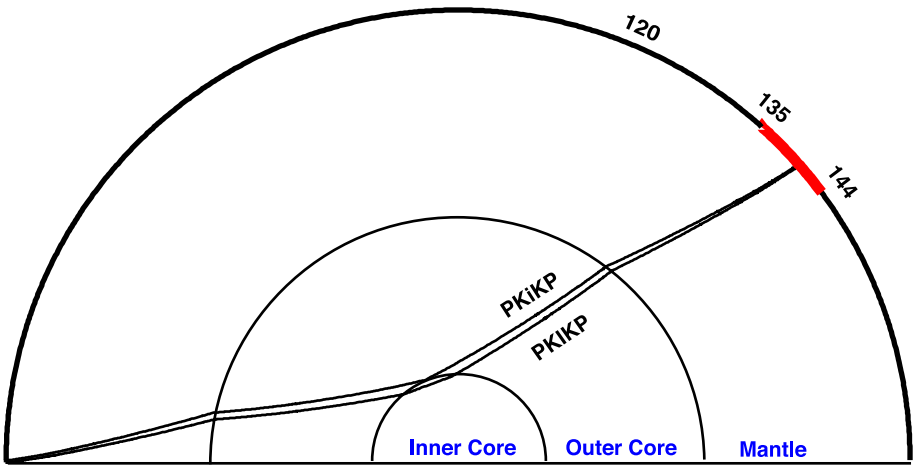

Fig. 1. Ray paths of PKiKP (reflected P wave from the ICB) and PKIKP (P wave passing through the inner core). The two phases may appear simultaneously as early as 120°, but we can only obtain well-separated PKIKP and PKiKP phases in the epicentral distance range from 135° to 144°.

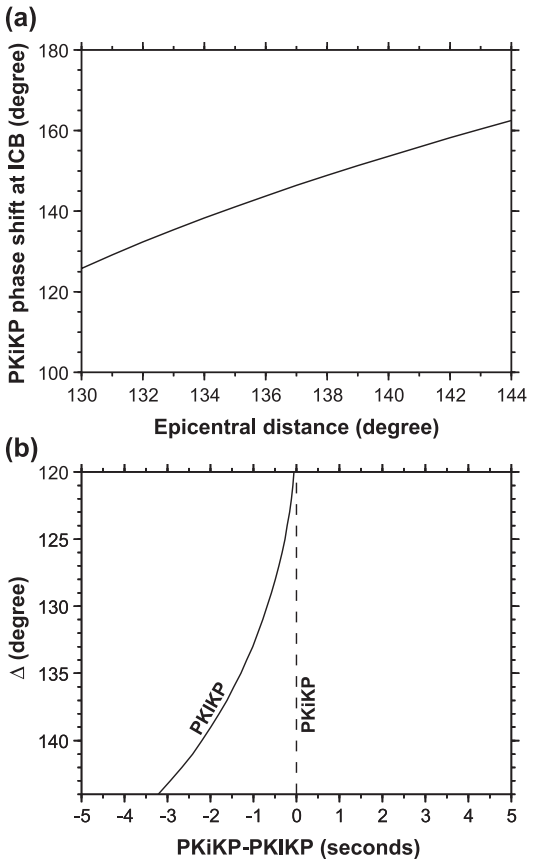

Fig. 2. (a) Phase shift of the post-critically reflected PKiKP with respect of PKIKP. (b) Differential travel time of PKIKP and PKiKP. The reference seismic model is PREM [28].

technique. However, because they chose different methods to deal with the problem of event source time functions and directivities, their estimations of Q_α are significantly different (at least by a factor of 3). In this paper, we will present a direct, but arguably effective, approach to circumvent the complex issue of event source time functions and directivities. We discuss the observed distribution of differential travel time residuals and amplitude ratios in terms of structure near the ICB.

2. Data, method, and results

We systematically downloaded both broadband and short-period vertical component seismograms from IRIS DMC, GRF, GRSN, Jarray, and F-net seismic networks corresponding to recordings in the epicentral distance range of 134–144°, for intermediate and deep earthquakes (focal depth >70 km, $M_w \geq 5.5$). These deeper events have shorter source time functions and higher signal-to-noise ratios than shallow events. To preprocess the seismograms, we employed a strictly narrow band-pass filter with corner frequencies of 0.7 and 2.0 Hz (corresponding to 1.5 and 0.5 s in period). The goal is to try to retrieve events whose 1.0 Hz energy was released in a short time and impulsively (within about 1.0 s), no matter how long their overall source time functions were. For this kind of events, we expect to observe pairs of well-separated PKIKP and PKiKP phases. Obtaining well-separated pairs of PKIKP and PKiKP phases requires us to apply a high frequency narrow band-pass filter. Therefore, we will not use the slope of amplitude spectrum ratio to estimate Q_α, as Souriau and Roudil [31] did, taking advantage of the broadband naturally well-separated PKIKP and PKPbc waveforms. In this paper, we directly measure amplitude ratios of PKIKP versus PKiKP in the time domain in order to estimate Q_α at the top of the inner core.

Our method requires to account for the phase shift of PKiKP with respect to PKIKP. Because PKiKP is a post-critically reflected wave at the ICB, the phase shift between PKiKP and PKIKP is approximately in the range of 142° to 163° (arguably close to 180°) in the epicentral distance range of our study (Fig. 2a). This means that if we reverse (that is multiplying the corresponding portion of the seismogram by −1) the PKiKP phase, the two phases should be very similar, as we verified using synthetic seismograms.

After data preprocessing, our data-picking criteria are as follows: (1) the signal-to-noise ratio before the identified PKIKP is ~6 or more; (2) the signal-to-noise ratio within about one duration of the waveform after the identified PKiKP is ~3 or more; (3) the identified PKIKP and PKiKP phases are well-separated; (4) the reversed PKiKP waveform is similar to the PKIKP waveform. Following the above criteria, we successfully selected 280 pairs of high-quality PKIKP and PKiKP phases (Fig. 3).

This large data set of well-separated and similar PKIKP and reversed PKiKP waveforms provides us a unique opportunity to explore the seismic structure at the top of the inner core. In order to study the P-wave velocity structure, we adopt two distinct methods to

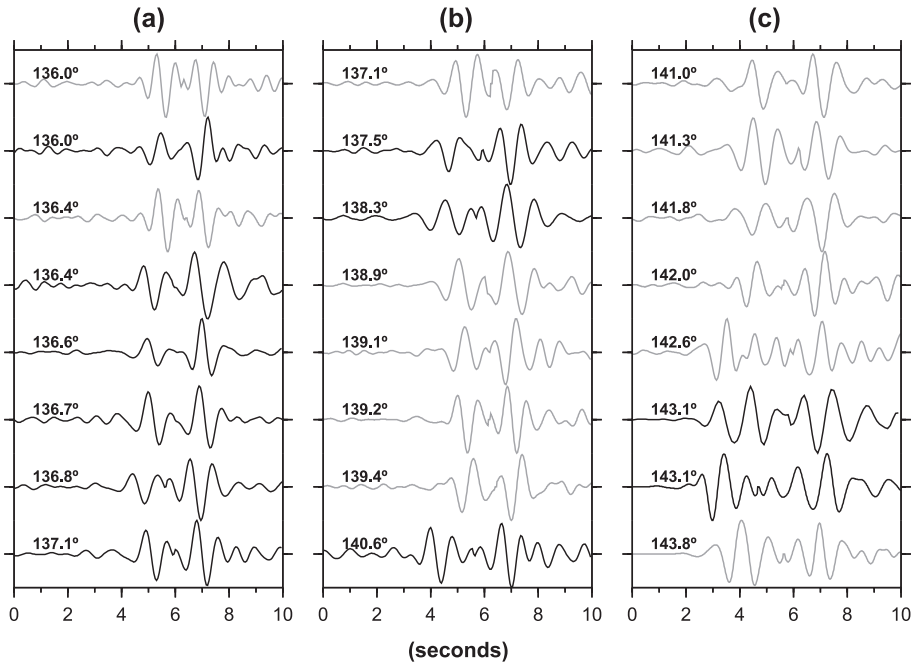

Fig. 3. Examples of well-separated PKIKP and reversed PKiKP phases. The original broadband or short period seismograms are filtered with a strictly narrow band-pass filter (around 1.0 Hz from 0.7 to 2.0 Hz). Grey traces are with PKIKP turning points in the western hemisphere, and black ones are with PKIKP turning points in the eastern hemisphere. In the distance range from 141° to 144° (panel c), we observe well-separated pairs of PKIKP and reversed PKiKP as both in the shorter (a) and longer (b) distance ranges.

measure the differential travel time between PKiKP and PKIKP. The first one is handpicking [21,23,34] before reversing PKiKP phases, and the second is cross-correlation after reversing PKiKP phases. Results from these two methods differ a little (less than ~0.1 s). Then we calculate the differential travel time residuals between PKiKP and PKIKP with respect to the reference seismic model PREM [28].

In order to study the Q_α structure, firstly, we measure the peak-to-peak amplitude ratios of PKIKP to PKiKP in the narrow band considered. Our measurements are carried on with Seismic Analysis Code (SAC). The measurement error of these amplitude ratios is negligible. Thus any possible source of random error should be related to the background noise. Our strict criteria of selection above can help us reduce this kind of random error significantly.

Secondly, we apply geometrical spreading, transmission, and reflection corrections for the measured amplitude ratios [35], based on the reference seismic model PREM [28]. The ratios of PKIKP and PKiKP geometrical spreading factors are functions of take-off angles, ray parameters, and their corresponding derivatives. The transmission and reflection coefficients are calculated with respect to various discontinuities (solid–solid, solid–liquid, and liquid–solid) in the earth.

Finally, we directly estimate Q_α from corrected amplitude ratios according to the definition of the seismic attenuation in the time domain:

$$\frac{A_{\mathrm{PKIKP}}}{A_{\mathrm{PKiKP}}} = e^{-\pi f t/Q_\alpha}$$

where A_{PKIKP} and A_{PKiKP} are the corrected amplitudes for PKIKP and PKiKP, respectively; t is the travel time of PKIKP in the inner core; f is the frequency, and Q_α is the quality factor which characterizes the seismic attenuation at the top of the inner core. Although, theoretically, the phase shift between PKIKP and PKiKP does not affect the measurement of amplitude ratios, we verified this in an experiment. We computed a series of phase shifted waveforms (140°, 145°, 150°, 155°, 160°, and 180°, respectively) with respect to an observed PKIKP phase. The

resulting variations of amplitude ratios are ~0.01, which is too small to cause a noticeable change of the estimated Q_α.

The uncertainty of our Q_α estimations can be divided into random and systematic errors. The systematic error is related to the reference seismic model. When we estimated Q_α using AK135 [36] and PREM2 [37] instead of PREM model, results are very compatible. The difference between Q_α estimated from AK135 and PREM2 is less than ± 10, and both estimates are consistently higher (~30) than those estimated from PREM model. In these three models, P-wave velocity contrasts (or sharpness) at the ICB and seismic structure near (both above and below) the ICB are rather different, but their influence on our Q_α estimations are small.

As for the random error (corresponding to our first step), an ideal way to estimate it is to use a number of different events in similar locations recorded by the same stations. Unfortunately, we do not have this kind of data. Thus we try to estimate standard deviations by distinguishing three cases: (1) in the epicentral distance range from 142° to 144°, we directly estimate a standard deviation ~43; (2) in the shorter epicentral distance range, we look for the regions where azimuths, sampling depths, and turning points of PKIKP are close (~2°×2°) in the eastern hemisphere. We obtain an average standard deviation ~24. (3) Similarly, in the western hemisphere, we obtain an average standard deviation ~50. These estimated standard deviations cannot be completely attributed to the background noise because of the likely

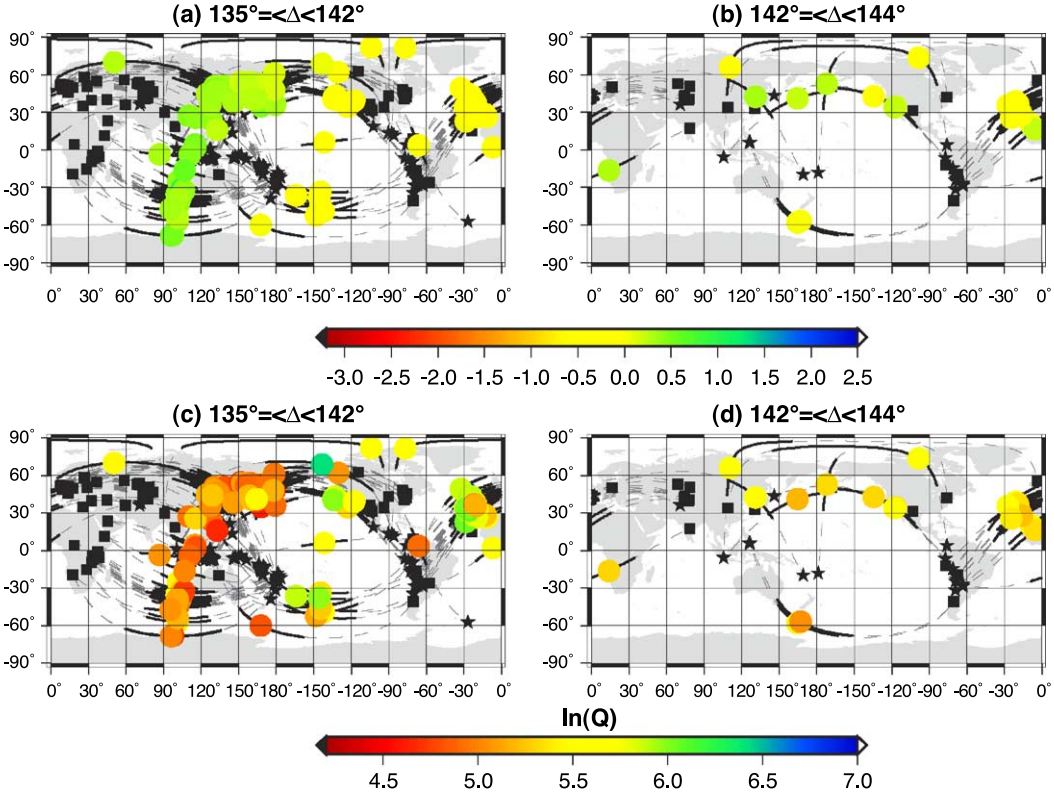

Fig. 4. Geographical distribution of differential travel time residuals between PKiKP and PKIKP and estimations of Q_α (referring to seismic model PREM [28]). (a) and (c) show clear hemispherical patterns of residuals and Q_α, respectively, in the epicentral distance range from 135° to 142° (corresponding to ~32 to ~85 km beneath the ICB). (b) and (d) show that hemispherical patterns disappear deeper than ~85 km beneath the ICB. Dashed lines are ray paths from events (stars) to stations (squares), and the bold lines are the inner core portion of PKIKP ray paths. The circles are the turning points of PKIKP in the inner core.

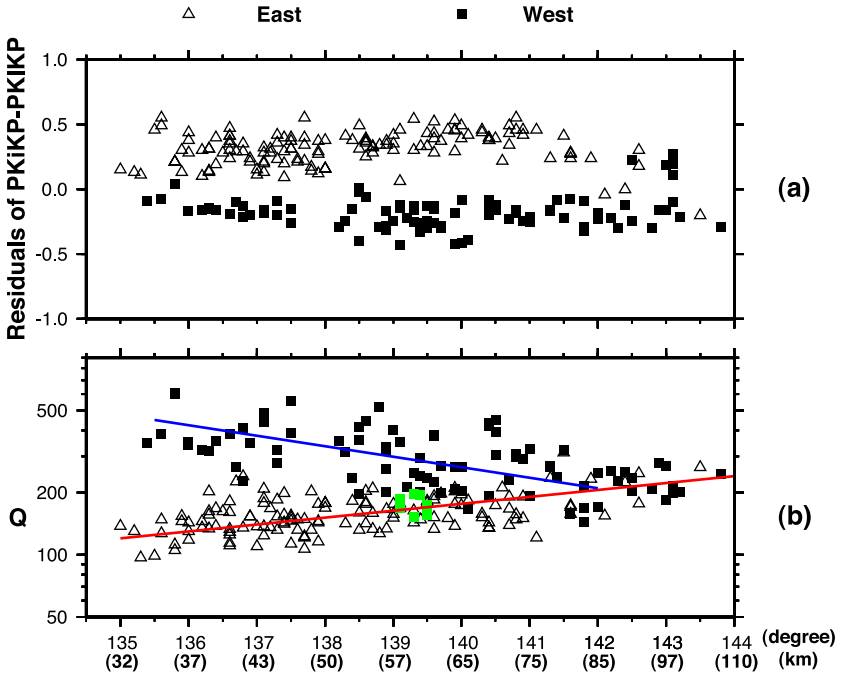

Fig. 5. (a) Differential travel time residuals (referring to PREM [28]). The measurement error is less than ~0.1 s. (b) Q_α with respect to the epicentral distance and depth beneath the ICB. The average standard deviations are from ~24, ~43, to ~50. Highlighted green squares show the data sampling offshore northwest of Africa. The event epicentral distances were all calibrated with a reference focal depth of 100 km.

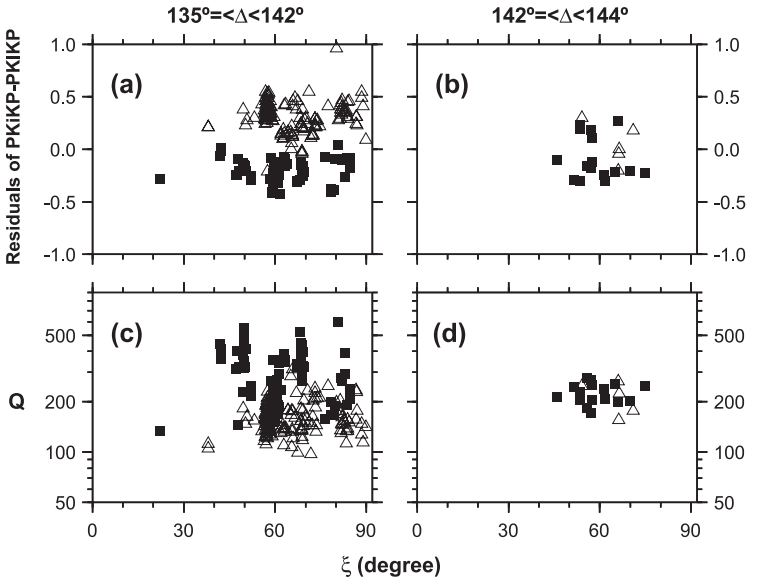

Fig. 6. Differential travel time residuals between PKiKP and PKIKP and Q_α versus ξ (ray angle of PKIKP with respect to the Earth's spin axis), respectively.

contribution from small-scale heterogeneity at the top of the inner core.

For differential travel time residuals, our results show a striking hemispherical pattern in the epicentral distance range 135° to 142° (corresponding to depths of approximately 32 to 85 km beneath the ICB) (Figs. 4a and 5a), in agreement with the observations of Niu and Wen [21] and Garcia [22]. Beyond 142°, the hemispherical pattern is not as clear (Fig. 4b).

For the quality factor Q_α, our results also show a reliable hemispherical pattern almost in the same epicentral distance range (135–141.5°) (Figs. 4c and 5b). In the western hemisphere, Q_α steadily decreases as a function of distance, with a mean of about 335 ± 50 which is lower than Niu and Wen's [21] estimate (Q_α~600).

In the eastern hemisphere, Q_α increases as a function of distance, with a mean of about 160, which is also lower than Wen and Niu's [23] estimate (Q_α~250). In the distance range overlapping that of Garcia [22] (from 135° to 136°), the mean of Q_α is about 125 ± 24, which is relatively compatible with his values (<100).

Beyond an epicentral distance of 141.5°, the hemispherical pattern in Q_α disappears (Figs. 4d and 5b), as does that in the differential travel time residuals. The Q_α measurements are consistent with a mean of 210 ± 43. This value is compatible with Souriau and Roudil's [31] estimate (Q_α~200).

We also examine the variation of Q_α versus ξ (PKIKP ray angle with respect to the Earth's spin axis) and differential travel time residuals versus ξ, respectively (Fig. 6). Our observations do not show any evidence for seismic anisotropy; however, our range of ξ is too limited to draw any definitive conclusions.

3. Discussion

3.1. Measurement robustness

In comparison with the method of waveform modeling, our approach has several advantages. We do not have to consider source time functions, directivities, and station-sided crustal structure, which are usually regarded as the main source of the uncertainty in the Q_α measurement [22]. In comparison with the method of amplitude ratio of PKIKP versus PKPbc, which is used at larger distance and therefore samples deeper in the inner core, the sampling depth range of PKIKP is much closer to the ICB and so the revealed seismic structure may be more directly related to the freezing process at the ICB. Also, the entry (and exit) points of PKIKP and PKiKP into the core at the CMB are much closer (less than ~120 km) than those of PKIKP and PKPbc (from ~210 to ~550 km). The two phases PKIKP and PKiKP are so close that we may assume that they are affected in the same way by heterogeneities in the crust, mantle, and even the outer core. If we assume a 10% velocity perturbation at the base of the D″, its influence on our estimation of Q_α is less than 1%. On the other hand, for the reflection of PKiKP at the ICB, if we assume a 5% velocity change (keeping its super critical reflection), the coefficient variation is also less than 1%, and so resulting influence on Q_α estimations is negligible. Finally, the difference in take-off angle between PKIKP and PKiKP at the source is significantly smaller (less than 1.5°) than that between PKIKP and PKPbc (from ~3.0° to ~6.0°). So the uncertainty related with the P-wave radiation pattern can be more confidently ignored in our estimation of Q_α.

The noise sources for our measurements are mainly the random background noise near stations, PKP precursors scattered in the mantle [39], and the possible interference with the PKPbc phase beyond an epicentral distance of 141°. The reference seismic model PREM [28], IASP91 [38], and AK135 [36] all predict that PKPbc does not appear until 144.5°, but it has been pointed out that in practice PKPbc might be observed as early as at the epicentral distance of 141° [31]. We believe our strict data picking criteria can effectively avoid the possible influence from the unexpected PKPbc in our range of study and expand the distance range of PKiKP versus PKIKP to the epicentral distance of 144°: (1) the waveforms of PKIKP and PKPbc are very similar. Once the PKPbc starts to appear, its travel time should be very close to that of PKIKP, and so a strong constructive interference usually happens. (2) In our epicentral distance range of study, the travel time difference of PKIKP and PKiKP is at most 3.2 s. If PKPbc appears between PKIKP and PKiKP we could not identify two almost completely separated phases. (3) If PKPbc arrives

closer to PKiKP, the two phases would destructively interfere with each other. Consequently, no PKiKP could be identified. (4) The most important point is that we are always looking for two well-separated phases and the latter one is almost reversed in polarity with respect to the first one. Therefore, as we showed in Fig. 3c, we cannot wrongly identify PKPbc as PKiKP even if it might occasionally appear before 144°. In fact, the potential PKPbc in our range of study is most likely a kind of low frequency diffracted wave near B cusp (Cormier, personal communication). After our relatively high frequency filtering, it will not to affect our identification of PKiKP.

The energy level of scattered PKP precursors is usually ~10% of the PKIKP's [39]. Sometimes they are hard to be discerned from the background noise without stacking and sometimes they are clear even in single station traces. Our required signal-to-noise ratios may help us limit the influence of both background noise and anomalous PKP precursors. Also, the requirement of similarity of PKIKP and reversed PKiKP phases further reduces the influence of noise through our data selection.

Although we employ a strictly narrow filter, we cannot obtain any well-separated pairs of PKIKP and PKiKP phases in the epicentral distance range from 134° to 135°. Our observations show that the duration of the PKIKP waveform is usually longer than 1.3 s (Fig. 3), which is larger than the predicted differential travel time between PKIKP and PKiKP in the distance range less than 135°. So the interference is a significant issue when using PKIKP and PKiKP phases to study the structure at the very top of the inner core [33,22]. It is possible to measure the differential travel time of the interfering phases of PKIKP and PKiKP using waveform modeling, but it seems very difficult to accurately measure the amplitude ratio of PKIKP versus PKiKP. Garcia [22] and Wen and Niu [23] used distinct methods to do the waveform modeling of PKIKP and PKiKP. They both proposed a hemispherical pattern for P-wave velocity but they obtained incompatible estimates of Q_α in the eastern hemisphere (by a factor of more than 3.0). In the epicentral distance range (135° to 136°), our estimate of Q_α in the eastern hemisphere is closer to Garcia's [22] result. This suggests to us that the direct consideration of source time functions and directivities is important for PKIKP and PKiKP waveform modeling due to the likely interference of these phases in a broadband sense. On the other hand, our Q_α measurements are compatible with Souriau and Roudil's [31] broadband estimates in the overlapping distance range (142° to 144°), further adding confidence in our results.

3.2. Interpretation

Our observations not only present additional evidence for a seismically isotropic hemispherical structure (high velocity low Q_α in the eastern hemisphere and low velocity high Q_α in the western hemisphere) at the top of the inner core [21–23], but also further indicate that this hemispherical isotropic structure disappears at a depth of about 85 km beneath the ICB. The most intriguing point is that our observation of Q_α provides evidence for a pronounced transition region of seismic attenuation at the top of the inner core, with hemispherical differences (Fig. 7).

So far, both scattering related with the iron crystal structure [40] and diffusion related with liquid inclusion [11] can account for previous observations that Q_α increases with depth (deeper than 100 km) [30–32]. As for which is the dominant factor, it is still an unsettled issue. Possibly this question depends on

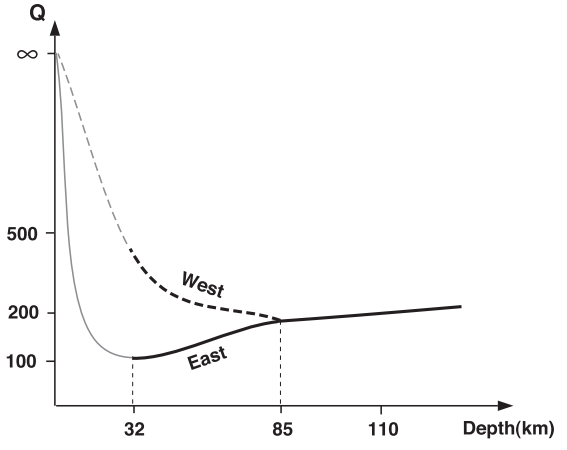

Fig. 7. Cartoon diagram of the hemispherical transition of seismic attenuation at the top of the Earth's inner core, where Q_α turns from decreasing to increasing with depth. Our sampling range is approximately from 32 to 110 km. In the deeper depth range, the increase of Q_α with respect to depth was suggested by a number of previous studies [31]. The grey thinner lines in the shallower depth range are inferred from our observation and Stroujkova and Cormier's [34] result.

the depth range of study. Cormier and Li [41] suggested that the inner core can be roughly divided into three sections based on iron crystal texturing: perfectly aligned deep part, incomplete aligned upper part, and a mushy zone at the top of the inner core. In the mushy zone, there would be significant exchange of fluid with the outer core because the estimated mushy zone Rayleigh number is at least one thousand times supercritical [40]. In what follows, we discuss our results under the assumption that the mushy zone exists, although alternative interpretations could be sought in terms of solid state texture effects. The mushy zone at the very top of the inner core may exhibit lateral variations in its melt fraction content, related to possible differences in heat flow near the ICB induced by lateral variations in temperature at the CMB. In the mushy zone, it is reasonable to assume that the porosity (or melt fraction) decreases with depth, due to the compaction of the solid–liquid composite resulting from expulsion of liquid towards the outer core [9,10]. Singh et al.'s [11] experiment, in which they assume that melt inclusions are not connected to each other, explicitly demonstrates that Q_α decreases as a function of the increasing melt fraction. Based on their experiment, we can readily infer that Q_α should increase with depth.

In the eastern hemisphere, at least up to 32 km beneath the ICB (the upper limit of our sampling in the inner core), our Q_α estimates are compatible with such a model. In the western hemisphere, however, the behavior is different. From ~32 to ~85 km beneath the ICB, Q_α decreases from ~335 to ~210. We suggest that in the western hemisphere porosity is higher and melt inclusions are connected and exchange fluid with the outer core [40], resulting in higher Q_α. P-wave velocity may, in turn, be reduced. Nevertheless, the well-linked or concentrated liquid may not be distributed evenly in the western hemisphere. In some regions (for example, the offshore northwest of Africa) or other yet unsampled areas (Figs. 4c and 5b), there may be well-isolated liquid inclusions.

The contrast between high Q_α and low P-wave velocity in western hemisphere and low Q_α and high P-wave velocity in the eastern hemisphere most likely reflects significant hemispherical difference of the freezing rate at the ICB. Sumita and Olson [42] suggest that a thermally heterogeneous mantle could control the convection in the liquid outer core and result in different heat flow near the ICB. On the cold western side, the rapid freezing might lead to higher porosity.

The disappearance of the hemispherical pattern in Q_α suggests to us that there is no significant difference in the nature of liquid inclusions in the two hemispheres within the depth range from ~85 to 110 km. In consequence, the resulting contributions to attenuation, due to the thermal and material diffusion [9], are basically compatible (Fig. 5b). However, the more scattered differential travel time residuals (Fig. 5a) imply that the perturbation of velocity in this depth range cannot be controlled by the texturing difference of liquid inclusions as in the upper portion of the top of the inner core. At this time, we have too few travel time measurements at distances greater than 142° to propose a unique interpretation of this scatter.

4. Conclusion

Our estimations of Q_α at the top of the inner core strongly suggest the existence of a transition zone of the seismic attenuation in the western hemisphere, where Q_α first decreases from almost infinite [27] at the ICB to ~210 at about 85 km beneath the ICB and then increases with depth into the inner core [31]. In the eastern hemisphere, we do not directly observe the transition but we infer that it must be located in the top 32 km of the inner core, which is supported by Stroujkova and Cormier's [34] most recent result that there is a low velocity layer in the upper most inner core in this region. The observed striking hemispherical pattern in seismic attenuation is presumably related to the melt fraction and the connectivity of the liquid inclusions. We infer that the liquid inclusions may be well isolated in the eastern hemisphere, while in the western hemisphere, they are better connected (as a result, the porosity is also higher). This kind of hemispherical pattern is probably caused by hemispherical temperature differences at the ICB [42]. On the cold western side, a faster freezing rate of the liquid material at the ICB can lead to higher porosity.

Our measurements of differential travel time residuals of PKiKP versus PKIKP confirm the existence of a hemispherical pattern of the isotropic P-wave velocity at the top of the inner core [21,22]. Low velocity, high Q_α, and high porosity are present

in the western hemisphere, and high velocity, low Q_α, and low porosity, respectively, in the eastern hemisphere.

However, the hemispherical patterns of Q_α and P-wave velocity cannot extend very deep into the inner core. Both of them disappear almost simultaneously ~85 km beneath the ICB. Below this depth, as Creager [18] suggested, the isotropic average velocities may be the same in both hemispheres.

Acknowledgements

Thanks to the following networks and data centers for providing the high quality data used in this study: IRIS-DMC, GRF, GRSN, J-array, and Fnet. We are grateful to Vernon Cormier for giving us their preprint, and Ikuro Sumita for discussion. This is BSL contribution #04–10.

References

[1] J.A. Jacobs, The earth's inner core, Nature 172 (1953) 297.
[2] F.D. Stacey, The cooling earth: a reappraisal, Phys. Earth Planet. Inter. 22 (1980) 89–96.
[3] S.I. Braginsky, Structure of the F layer and reasons for convection in the earth's core, Dokl. Acad. Sci. USSR., Engl. Transl. 149 (1963) 8–10.
[4] F. Birch, Density and composition of the mantle and core, J. Geophys. Res. 69 (1964) 4377–4388.
[5] D. Gubbins, Energetics of the earth's core, J. Geophys. 43 (1977) 453–464.
[6] D.E. Loper, The gravitationally powered dynamo, Geophys. J. R. Astr. Soc. 54 (1978) 389–404.
[7] D. Gubbins, D. Alfe, G. Masters, G.D. Price, M.J. Gillan, Can the earth's dynamo run on heat alone? Geophys. J. Int. 155 (2003) 609–622.
[8] D.R. Fearn, D.E. Loper, P.H. Roberts, Structure of the earth's inner core, Nature 292 (1981) 232–233.
[9] D.E. Loper, D.R. Fearn, A seismic model of partially molten inner core, J. Geophys. Res. 88 (1983) 1235–1242.
[10] I. Sumita, S. Yoshida, M. Kumazawa, Y. Hamano, A model for sedimentary compaction of a viscous medium and its application to inner-core growth, Geophys. J. Int. 124 (1996) 502–524.
[11] S.C. Singh, M.A.J. Taylor, J.P. Montagner, On the presence of liquid in Earth's inner core, Science 287 (2000) 2471–2474.
[12] A. Morelli, A.M. Dziewonski, J.H. Woodhouse, Anisotropy of the inner core inferred from PKIKP travel times, Geophys. Res. Lett. 13 (1986) 1545–1548.
[13] J.H. Woodhouse, D. Giardini, X.D. Li, Evidence for inner core anisotropy from free oscillations, Geophys. Res. Lett. 13 (1986) 1549–1552.
[14] L. Vinnik, B. Romanowicz, L. Bréger, Anisotropy in the center of the inner core, Geophys. Res. Lett. 21 (1994) 1671–1674.
[15] X. Song, Anisotropy in central part of inner core, J. Geophys. Res. 101 (1996) 16089–16097.
[16] T.J. McSweeney, K.C. Creager, R.T. Merrill, Depth extent of inner-core seismic anisotropy and implications for geomagnetism, Phys. Earth Planet. Inter. 101 (1997) 131–156.
[17] S. Tanaka, H. Hamaguchi, Degree one heterogeneity and hemispherical variation of anisotropy in the inner core from PKP(BC)–PKP(DF) times, J. Geophys. Res. 102 (1997) 2925–2938.
[18] K.C. Creager, Large-scale variations in inner core anisotropy, J. Geophys. Res. 104 (1999) 23127–23139.
[19] A. Souriau, B. Romanowicz, Anisotropy in inner core attenuation: a new type of data to constrain the nature of the solid core, Geophys. Res. Lett. 23 (1996) 1–4.
[20] S.I. Oreshin, L.P. Vinnik, Heterogeneity and anisotropy of seismic attenuation in the inner core, Geophys. Res. Lett. 31 (2004) L02613.
[21] F. Niu, L. Wen, Hemispherical variations in seismic velocity at the top of the Earth's inner core, Nature 410 (2001) 1081–1084.
[22] R. Garcia, Constraints on upper inner-core structure from waveform inversion of core phases, Geophys. J. Int. 150 (2002) 651–664.
[23] L. Wen, F. Niu, Seismic velocity and attenuation structures in the top of the Earth's inner core, J. Geophys. Res. 107 (2002) 2273.
[24] B. Romanowicz, H. Tkalcic, L. Bréger, On the origin of complexity in PKP travel time data from broadband records, in: V. Dehant, K. Creager (Eds.), Earth's Core: Dynamics, Structure, Rotation, AGU Geodynamics Series, vol. 31, 2002, pp. 31–44.
[25] M. Ishii, A.M. Dziewonski, J. Tromp, G. Ekstrom, Joint inversion of normal mode and body wave data for inner core anisotropy: 2. Possible complexities, J. Geophys. Res. 107 (2002) 2380.
[26] L. Bréger, H. Tkalcic, B. Romanowicz, The effect of D″ on PKP(AB-DF) travel time residuals and possible implications for inner core structure, Earth Planet. Sci. Lett. 175 (2000) 133–143.
[27] V.F. Cormier, P.G. Richards, Comments on 'The damping of the core waves' by Antony Qammar and Alfredo Eisenberg, J. Geophys. Res. 981 (1976) 3066–3068.
[28] A.M. Dziewonski, D.L. Anderson, Preliminary reference earth model, Phys. Earth Planet. Inter. 25 (1981) 297–356.
[29] J. Bhattacharyya, P. Shearer, G. Masters, Inner core attenuation from sort period PKP(BC) versus PKP(DF) waveforms, Geophys. J. Int. 114 (1993) 1–11.
[30] X. Song, D.V. Helmberger, Depth dependence of anisotropy of the Earth's inner core, J. Geophys. Res. 100 (1995) 9805–9816.

[31] A. Souriau, P. Roudil, Attenuation in the uppermost inner core from broad-band GEOSCOPE PKP data, Geophys. J. Int. 123 (1995) 572–587.
[32] X. Li, V.F. Cormier, Frequency-dependent seismic attenuation in the inner core: 1. A viscoelastic interpretation, J. Geophys. Res. 107 (2002) 2361.
[33] V.F. Cormier, G.L. Choy, A search for lateral heterogeneity in the inner core from differential travel times near PKP-D and PKP-C, Geophys. Res. Lett. 13 (1986) 1553–1556.
[34] A. Stroujkova, V.F. Cormier, Regional variations in the uppermost 100 km of the Earth's inner core, J. Geophys. Res. 109 (2004) DOI:10.1029/2004JB002976.
[35] A. Cao, B. Romanowicz, Constraints on density and shear velocity contrasts at the inner core boundary, Geophys. J. Int. 157 (2004) 1146–1151.
[36] B.L.N. Kennett, E.R. Engdahl, R. Buland, Constrains on seismic velocities in the Earth from travel times, Geophys. J. Int. 122 (1995) 108–124.
[37] X. Song, D.V. Helmberger, A P wave velocity model of Earth's core, J. Geophys. Res. 100 (1995) 9817–9830.
[38] B.L.N. Kennett, E.R. Engdahl, Travel times for global earthquake location and phase identification, Geophys. J. Int. 105 (1991) 429–465.
[39] M.A.H. Hedlin, P.M. Shearer, P.S. Earle, Waveform stacks of PKP precursors: evidence for small-scale heterogeneity throughout the mantle, Nature 387 (1997) 145–150.
[40] M.I. Bergman, Solidification of the Earth's core, in: V. Dehant, K.C. Creager, S. Karato, S. Zatman (Eds.), Earth's Core: Dynamics, Structure, Rotation, AGU Geodynamics Series, vol. 31, 2002, pp. 105–127.
[41] V.F. Cormier, X. Li, Frequency-dependent seismic attenuation in the inner core: 2. A scattering and fabric interpretation, J. Geophys. Res. 107 (2002) 2362.
[42] I. Sumita, P. Olson, A laboratory model for convection in Earth's core driven by a thermally heterogeneous mantle, Science 286 (1999) 1547–1549.